

# The Effect of Adding a Square Disturbance on the Flow Characteristics across Circular Cylinders Arranged in Tandem

Novi Indah Riani<sup>a,\*</sup>, Aini Lostari<sup>a</sup>, Miftahul Ulum<sup>a</sup>, Ainul Hakim<sup>a</sup>

<sup>a</sup> Department of Mechanical Engineering, University of Qomaruddin, Jl. Raya Bungah No. 1, Gresik 61152, Indonesia  
e-mail: [noviindahriani@gmail.com](mailto:noviindahriani@gmail.com)\*, [ainims31@gmail.com](mailto:ainims31@gmail.com), [ulum@uqgresik.ac.id](mailto:ulum@uqgresik.ac.id).

## Keywords:

Circular cylinder,  
Square Disturbance  
Body, Tandem, Flow  
Characteristic.

## ABSTRACT

Circular cylinder is one form of bluff body that is often used in engineering and industrial applications. The addition of a square placed in front of the circular cylinder aims to accelerate the flow from laminar to turbulent so that flow separation can be delayed more slowly so that the resulting pressure drag is smaller. The research method used was experimental using two circular cylinders arranged in tandem with a diameter ( $D$ ) of 25 mm and variations in the distance between cylinders ( $L/D$ ) 2;2,5;3;3,5;4 and two square-shaped square bodies (SDB) in front of each cylinder with dimensions of 4 mm. Position of SDB angle is  $30^\circ$  and the gap distance is 0.4 mm. The Reynolds number used is  $2.3 \times 10^4$ . This study aims to obtain the distribution of pressure coefficient (CP), drag pressure coefficient (CDP) and velocity profile behind the test specimen. The results showed that the addition of two square-shaped square bodies on each cylinder can reduce the drag force on the cylinder which causes a difference in values, where the largest pressure coefficient value occurs at a distance of  $L/D$  4 with a value of -1.073 and the lowest value of drag pressure coefficient (CDP) at a distance of  $L/D$  2 on the upstream cylinder with a value of 0.0786. While the downstream cylinder is located at a distance of  $L/D$  3 with a value of -0.079 and the lowest speed value is located in the variation of  $L/D$  4 with a value of 9.52 m/s.

## 1. INTRODUCTION

Circular cylinders are a form of bluff body that is commonly used in engineering applications [1]. Circular cylinders result in normal stress and shear stress. Interaction between fluid flow with bluff body geometry or streamlined body, where the boundary layer is transformed from laminar flow to turbulent flow [2-3].

The addition of interference to the front of the main cylinder aims to accelerate the more turbulent flow so that the resulting pressure drag will be smaller. It's because of the delayed flow separation. Some previous research has been a reference to the reduction of the barrier style. One was performed by Tang, dkk [4] where he performed a simulation near the wall on a tandem arrangement with a low Reynolds number. Besides, Igarashi and Shiba [5] put the intruder in front of the main cylinder in a tandem position. Then Prasad and Williamson [6] used a flat plate of a certain dimension placed in front of the main cylinder vertically and horizontally against the direction of flow. Not only the addition of interference, but the various forms of arrangement as well as the main cylinder spacing also influence the value of the pressure drag [7-12].

Other research by Daman and Widodo on the addition of the Inlet Disturbance Body (IDB) to a circular cylinder that is arranged in tandem shows that bubble separation occurs in the circular Cylinder given the IDB. The separation point is at  $115^\circ$ , while cylinders without IDB are at  $90^\circ$  [13]. Other research has been done by adding IDB to circular cylinders that are arranged inline square. The results show that at the distance ratio  $L/D$  2 produces a narrow wake or a small shock deficit so that the separation is more delayed backwards. Then the reduction of the drag pressure coefficient (CDP) was obtained for cylinder 1 by 2.55 cylinders 2,796, cylinder 3 by -0.28 and cylinder 4 by 0.02 [14]. The interference shape also affects the characteristic result of the flow passing through a circular cylinder.

Square-shaped interferences have also been studied by several previous researchers. One of them was Rina and Ardhy in 2018 [15]. The study used a 4 mm square interference body placed in front of a circular cylinder that was arranged in tandem. The results show that adding downstream cylinders can contribute to reducing the drag style of upstream cells using a square disturbance body. The effect of the upstream wake cylinder on the downstream cylinders decreases with the increasing  $L/D$  ratio. The upstream and downstream wake interaction occurs in the  $1.5\text{--}3 L/D$  configuration.

Based on previous research, it proved that with the addition of interference either cylindrical, square, elliptical or other shapes can delay the separated flow further backwards. But in tandem arrangements, there has been no study of interference additions to each cylinder both in the upstream and in the downstream cylinders. The research will be conducted experimentally using wind tunnels by varying the distance between circular cylinders ( $L/D$ ) arranged in tandem with the aim of finding out the flow characteristics including pressure drag values, drag coefficients and velocity profiles behind the circular cylinder.

## 2. METHODS

### 2.1 Research Design

The test object is a circular cylinder arranged in tandem with a diameter width of  $D = 25$  mm with the addition of two square-shaped interference bodies on each of the cylinders with sides of 4 mm and the gap between interferences with the circular cylinder of 0.4 mm, as well as the interference angle towards the center of the circular cylinder of  $30^\circ$ . As for the material of the circular cylinder and the interferences are made of PLA and acrylic. Wall-pressure taps are placed in the upstream and downstream parts of cylinders to obtain the pressure that occurs on the circular cylinder. The pitot tube is placed on the upstream side 100 mm away from the main cylinder axis, while the downstream side is  $4D$  away from upstream cylinders' axis. Here's the design of this study:

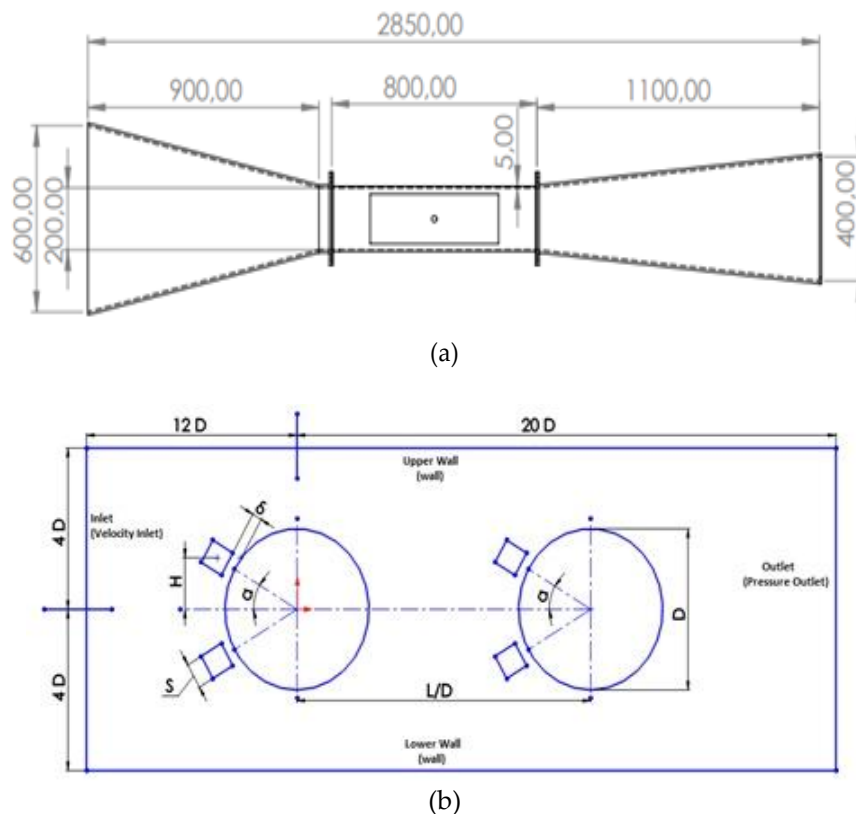


Figure 1. Research Design (a) Side View (b) Tandem Circular Cylinder Installation Details

Description:

D = Cylinder Diameter

s = SDB length

$\theta$  = SDB angle

S = Distance center to center between main cylinders (susunan tandem)

H = SDB center height with main cylinder center

$\delta$  = Gap between SDB and main cylinder

In this study, the value of the blockage ratio on the variation of the SDB angle = 30° is 12.5%.

$$\text{Blockage Ratio} = \frac{d}{h} \times 100\%$$

Where,

d = The diameter of the test object along the test section

h = Width test section

$$\begin{aligned} \text{Blockage Ratio} &= \frac{25 \text{ mm}}{200 \text{ mm}} \times 100 \\ &= 12,5\% \end{aligned}$$

Where,

25 mm = Circular cylinder diameter

200 = h

## 2.2 Data Retrieval Process

Before taking the data, it is necessary to calibrate the measuring device as well as the test section. Here are the calibration steps, among others:

1. The static tube pitot is mounted on the wall connected to the Arduino Uno
2. Measures the inverter from 15 – 45 Hz. With intervals of 15,20,25,30,35,40,45 Hz
3. Takes pressure data from the digital manometer and the flow speed obtained from the Arduino Uno.
4. The data that has been obtained will be used as a graph of the relationship between the current speed of the inverter and the flow speed.

After calibration, the steps in the data collection process are as follows:

1. Preparation of equipment and installation of test objects used for conducting research.
2. Measure the temperature of the indoor air during the test (temperature and atmospheric pressure).
3. Install the test object on the wind tunnel, i.e. two circular cylinders with a diameter of D = 25 mm arranged in tandem with a distance of L/D 2.5 and then an interference body with a side (s) = 4 mm positioned at an angle of 30° on the upstream.
4. Turn on the wind tunnel by adjusting the fan speed slowly using the inverter to steady conditions.
5. Measures the pressure along the surface of the cylinder mounted wall pressure tap using a digital manometer.
6. Record the flow speed value obtained from pitot tube reading using Arduino Uno. Data collection for flow speed profile can be seen in the image below:

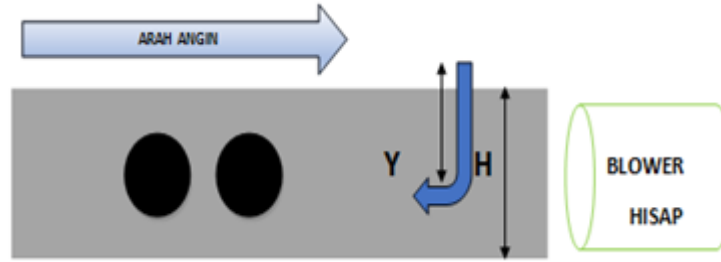


Figure 2. Data retrieval for Velocity Profile

Description:

Y = Interval distance of *pitot tube*

H = Height of *test section*

7. Disable the fan and reset the experimental installation.
8. Repeat data capture steps on each L/D distance variation.

Table 1. Data Collection for Variation of Cylinder Spacing to Pressure Values

Variation (L/D)	Angle	Air Velocity (m/s)	Static Pressure (kPa)	Dynamic Pressure (kPa)
2	30°			
2,5	30°			
3	30°			
3,5	30°			
4	30°			

Note:

To get the speed with each variation of the distance one is L/D 2.5 and angle 30°, the pitot tube is placed every 1 cm from the top of the test section to the bottom of the testing section.

### 2.3 Calculation Result Data

After taking the data, the data will be processed into the formula below:

The drag coefficient is divided into two, namely:

- a. *Pressure drag*, where the value is obtained from the presence of pressure
- b. *Skin friction drag*, the value is based on wall shear stress, but for this study skin friction drag has not been studied.

The calculation of the pressure drag coefficient ( $C_{DP}$ ) is obtained from the pressure distribution value ( $C_p$ ) of the result of integrating the pressure coefficient of the surface contour of the cylinder. ( $C_p$ ) [16].

$$C_{DP} = \frac{1}{2} \int_0^{2\pi} C_p(\theta) \cos(\theta) d\theta$$

Whereas to obtain the value of the pressure drag coefficient ( $C_{DP}$ ) can be solved by the numerical method of Simpson's 1/3 double segment rule which is formulated on the following equation:

$$I \cong (b - a) \frac{f(x_0) + 4 \sum_{i=1,3,5}^{n-1} f(x_i) + 2 \sum_{j=2,4,6}^{n-2} f(x_j) + f(x_n)}{3n}$$

Where:

- $b = 2\pi$  and  $a = 0$ ,  $f(x_0) = C_p(0) \cos(0)$  and  $f(x_n) = C_p(2\pi) \cos(2\pi)$  to solve dynamic pressure equations.
- $b = h$  and  $a = 0$ ,  $f(x_0) = u(y_0)$  and  $f(x_n) = u(y_n)$  to solve pressure coefficient equations ( $C_p$ ).
- $f(x_i)$  is the proliferation of the gasal data function where is  $i = 1, 3, 5 \dots n-1$ .
- $f(x_j)$  is the proliferation of the genap data function where is  $j = 2, 4, 6 \dots n-2$ .
- $n =$  amount of data

The integration used to obtain the pressure drag coefficient is the numerical integration of the Simpson method 1/3. The general equation is as follows:

$$\frac{1}{2} \int_a^b y(x) dx = \frac{b-a}{2 \times 3n} \{y_0 + 2(y_2 + \dots + y_{n-2}) + 4(y_1 + \dots + y_{n-1}) + y_n\}$$

So:

$$C_{Dp} = \frac{b-a}{2 \times 3n} \{y_0 + 2(y_2 + \dots + y_{n-2}) + 4(y_1 + \dots + y_{n-1}) + y_n\}$$

Where,

- $a$  = starting angle  
= 0
- $b$  = last angle  
=  $2\pi$
- $n$  = 72 ( $360^\circ : 5^\circ$ )
- $y_0$  = first data

$2(y_2 + \dots + y_{n-2}) =$  amount of genap data

$4(y_1 + \dots + y_{n-1}) =$  jumlah of ganjil data

$y_n =$  last data

Data analysis is done to obtain the desired results of the study, including flow speed, pressure distribution, and drag coefficient values passing through the test object. After that, discussions are conducted on the influence of the addition of square-shaped interference bodies with variations in the distance between cylinders to the flow speed values, the distribution of pressure, and the pressure drag values.

### 3. RESULTS AND DISCUSSION

#### 3.1 Distribution of pressure coefficients on upstream cylinders

Here is an example of the calculation of the distribution of the pressure coefficient at the variation  $L/D=2$  at the angle of the contour  $0^\circ$  (point of stagnation) [17]:

$$C_p = \frac{P_K - P_\infty}{\frac{1}{2} \rho U_\infty^2}$$

Where the value of  $\frac{1}{2} \rho U_{\infty}^2$  is the dynamic pressure obtained from the digital manometer during the data collection process.

$$C_p = \frac{(0,00 - (-0,138))kPa}{0,145 kPa} = 0,952$$

The value of the distribution of the pressure coefficient ( $C_p$ ) obtained in the tandem arrangement experimentally can be seen in Figure 3. The graph of each upstream cylinder with all the variations of  $L/D$  is shown in the figure below.

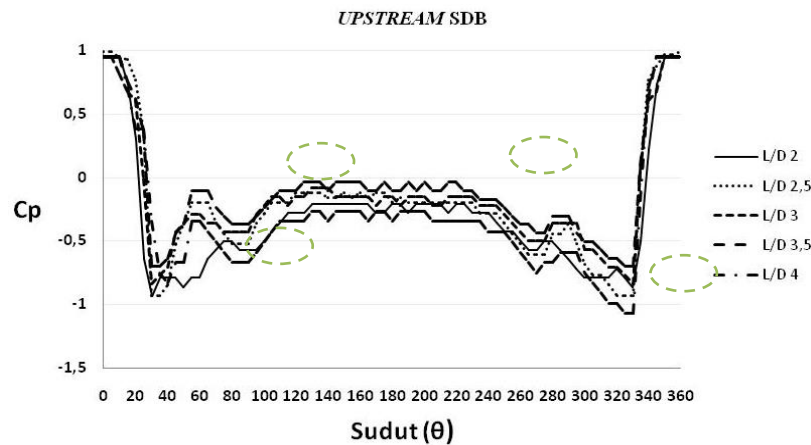


Figure 3. Comparison of All Upstream Cylinder Variations with SDB

The distribution of the pressure coefficient for all variations of  $L/D$  with the SDB at the upstream position, the stagnation point is at an angle of  $0^\circ$ . After the static point, the flow undergoes an acceleration characterized by an extreme decrease in the graph of pressure coefficients to the extent that the flow has a maximum speed characterized by the lowest pressure coefficient distribution value. On the upper side the flow occurs at the maximum speed at a angle of  $30^\circ$ , whereas on the lower side the stream undergoing the maximum velocity at the angle of  $230^\circ$ . Then the flow is slowed down due to the presence of adverse pressure characterized as an increase in pressure. At one point, it is no longer capable of resisting adverse pressures and friction, so there is a separation marked by pressure coefficients starting at a steady angle of  $90^\circ$  for the top and  $270^\circ$  for the bottom. The difference between each variation of the distance  $L/D$  is the highest peak at the distance  $L/D$  3.5 at the point of angle of contour  $60^\circ$ . The lowest value of the coefficient at the difference of distance  $L/D$  3 at the contour of  $30^\circ$  with a value of  $-0,927$  on the upper side and on the lower side located at the length  $L/D$  4 with a contour angle of  $330^\circ$  at the value  $-1,073$  then the maximum value is at the variation  $L/D$  3,5 at the contour of  $60^\circ$  with the value of  $+0,106$  at the position of upper sides and at the side lower side is at  $L/D$  3,5 with the angle of contour  $215^\circ$  with value of  $-0,040$ .

### 3.2 Distribution of pressure coefficients on downstream cylinder

A comparison of all downstream cylinder graphs with additional SDBs indicates that not all  $L/D$  variations at the position of the stagnation point at an angle of  $0^\circ$ . After the stasis point, the flow undergoes an acceleration characterized by an extreme decrease in the pressure coefficient graph to the extent that the flow has a maximum speed characterised by the lowest pressure factor distribution value. The difference of each variation of the  $L/D$  distance is seen at the lowest coefficient value at the variance of the  $L/D$  4 distance at the contour of  $30^\circ$  with a value of  $-0,911$  on the upper side and on the lower side located at the distance of  $L/D$  4 with a contour angle of  $330^\circ$  with the value of  $-0,911$  then the maximum coefficient value lies at the variant of  $L/D$  3.5 on

the contours of 180o with value of 0,262 in the position of the upper side and at the lower sides located on the L/D 2.5 with an angle of contour 330o at the value 0.282. Then the flow is slowed down due to an adverse pressure marked by an increase in pressure, this can be seen on the whole variation of L/D. At one point, the flow can no longer resist adverse pressures and friction so there is a separation marked by pressure coefficients starting steady at a 90° angle for the upper side and 270° for the lower side of the L/D 3 as seen in Figure 4.

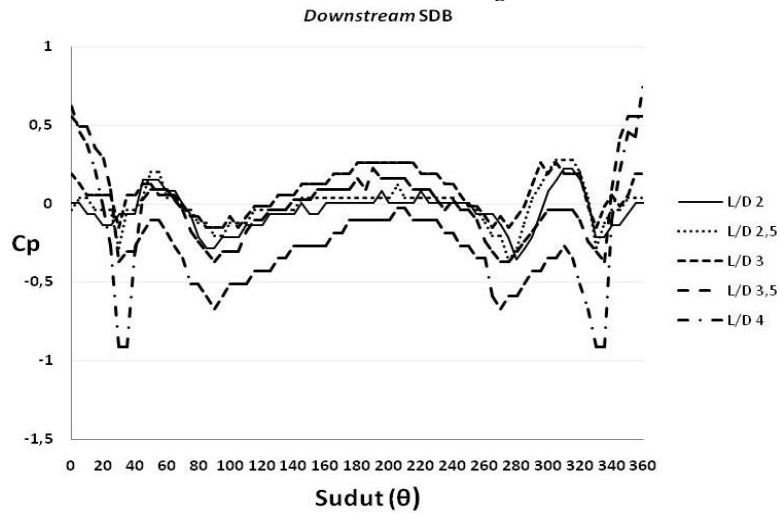


Figure 4. Comparison of All Upstream Cylinder Variations with SDB

### 3.3 Distribution of pressure coefficients on downstream cylinder

The speed profile behind the experimentally obtained cylinder configuration is shown in Figure 5. The result of the speed profile distribution shows that a tandem cylinders configuration with 30° SDB at a distance L/D 4 has the greatest momentum deficit marked by the lowest  $V/V_{max}$  value of approximately 0.583. This is because the flow that crosses the downstream cylinder is almost the same as the flow characteristics of the single cylinders so that the wake that occurs is the wake of the downstream, whereas at a narrower distance the wake occurs of the upstream that covers the downstream cylinder. Whereas the narrowest wake width occurs at the distance L/D 2.

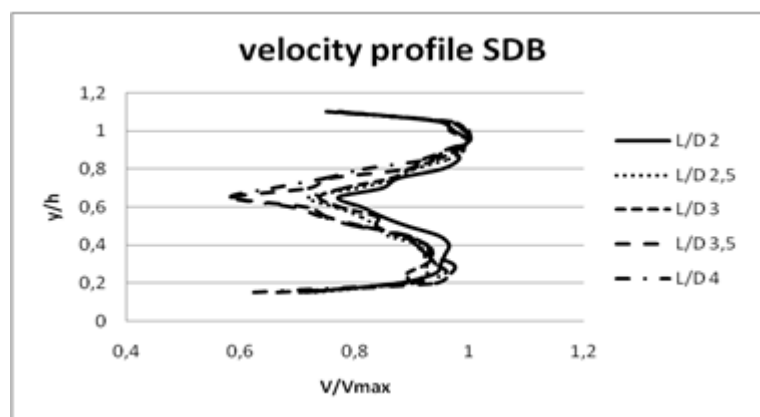


Figure 6. Velocity Profile

### 3.4 Distribution of pressure coefficients on downstream cylinder

The study also calculated the value of the drag pressure coefficient produced experimentally to find out what distance that produces the smallest drag pressure factor value to be able to reduce a better drag force.

The magnitude of the drag pressure coefficient against the Reynolds number is shown in table 2 below. Results obtained on two circular cylinders arranged in tandem based on the Reynolds number is  $2,3 \times 10^4$ .

Table 2. Value of Drag Pressure Coefficient with SDB

L/D	Upstream	Downstream
2	0,0786	-0,009
2,5	0,17089	-0,00742
3	0,1558	-0,0794
3,5	0,15288	0,0237
4	0,23616	0,03359

A drag coefficient is the measurement of an object's ability to withstand movement while fluid (air) flows, or the ability of a object to pass wind resistance. One way to reduce the obstacle or drag is to take into account the design of the test object. Besides, it can also add interference with various shapes on the front of the test object. From table 2 it can be seen that the smallest drag coefficient value is obtained on L/D 2 with SDB on the upstream part of the cylinder of 0,0786 whereas the largest Cd on L / D 4 with the value of 0,23616. This is because the closer the distance L/D is able to reduce the drag force better. While the downstream cylinder has a lower drag coefficient because the flow pressure has to pass the narrow wake of the upstream.

#### 4. CONCLUSION

Based on the results of research and data analysis, the conclusion of this study is that the distribution of pressure coefficients on tandem circular cylinder arrangements with the addition of square interference bodies varies each variation of L/D. But for the greatest reduction value of drag style obtained on variation L/D 2. While the maximum and minimum speed profiles occur at the L/D 4 variation.

#### REFERENCES

- [1] Derakhshandeh, J., & Alam, M. M. (2019, June). A review of bluff body wakes. *Ocean Engineering*, 182, 475–488. <https://doi.org/10.1016/j.oceaneng.2019.04.093>
- [2] Niemann, H. J., & Hölscher, N. (1990, March). A review of recent experiments on the flow past circular cylinders. *Journal of Wind Engineering and Industrial Aerodynamics*, 33(1–2), 197–209. [https://doi.org/10.1016/0167-6105\(90\)90035-b](https://doi.org/10.1016/0167-6105(90)90035-b)
- [3] Zdravkovich, M. (1990, March). Conceptual overview of laminar and turbulent flows past smooth and rough circular cylinders. *Journal of Wind Engineering and Industrial Aerodynamics*, 33(1–2), 53–62. [https://doi.org/10.1016/0167-6105\(90\)90020-d](https://doi.org/10.1016/0167-6105(90)90020-d)
- [4] Tang, G. Q., Chen, C. Q., Zhao, M., & Lu, L. (2015, October). Numerical simulation of flow past twin near-wall circular cylinders in tandem arrangement at low Reynolds number. *Water Science and Engineering*, 8(4), 315–325. <https://doi.org/10.1016/j.wse.2015.06.002>
- [5] Igarashi, T., & Shiba, Y. (2006). Drag Reduction for D-Shape and I-Shape Cylinders (Aerodynamic Mechanism of Reduction of Drag). *JSME International Journal Series B*, 49(4), 1036–1042. <https://doi.org/10.1299/jsmeb.49.1036>
- [6] Prasad, A., & Williamson, C. (1997, July). A method for the reduction of bluff body drag. *Journal of Wind Engineering and Industrial Aerodynamics*, 69–71, 155–167. [https://doi.org/10.1016/s0167-6105\(97\)00151-7](https://doi.org/10.1016/s0167-6105(97)00151-7)
- [7] Raiola, M., Ianiro, A., & Discetti, S. (2016, November). Wake of tandem cylinders near a wall. *Experimental Thermal and Fluid Science*, 78, 354–369. <https://doi.org/10.1016/j.expthermflusci.2016.06.003>
- [8] Chen, W., Ji, C., Xu, D., & Zhang, Z. (2020, April). Vortex-induced vibrations of two inline circular cylinders in proximity to a stationary wall. *Journal of Fluids and Structures*, 94, 102958. <https://doi.org/10.1016/j.jfluidstructs.2020.102958>



- 
- [9] Sisodia, S. S., Sarkar, S., & Saha, S. K. (2017, November). Fluid flow and mixed convective heat transfer around a semi-circular cylinder at incidence with a tandem downstream square cylinder in cross flow. *International Journal of Thermal Sciences*, 121, 13–29. <https://doi.org/10.1016/j.ijthermalsci.2017.06.027>
- [10] Li, L., Liu, P., Xing, Y., & Guo, H. (2019, September). Experimental investigation on the noise reduction method of helical cables for a circular cylinder and tandem cylinders. *Applied Acoustics*, 152, 79–87. <https://doi.org/10.1016/j.apacoust.2019.03.027>
- [11] Meneghini, J., Saltara, F., Siqueira, C., & Ferrari, J. (2001, February). Numerical Simulation Of Flow Interference Between Two Circular Cylinders In Tandem And Side-By-Side Arrangements. *Journal of Fluids and Structures*, 15(2), 327–350. <https://doi.org/10.1006/jfls.2000.0343>
- [12] Zhang, Z., Ji, C., Chen, W., Hua, Y., & Srinil, N. (2021, April). Influence of boundary layer thickness and gap ratios on three-dimensional flow characteristics around a circular cylinder in proximity to a bottom plane. *Ocean Engineering*, 226, 108858. <https://doi.org/10.1016/j.oceaneng.2021.108858>
- [13] Daman, A. A., & Widodo, W. A. (2014, Oktober). Pengaruh Penambahan *Inlet Disturbance Body* Terhadap Karakteristik Aliran Silinder Sirkular Secara Tandem. *Proceeding Seminar Nasional Tahunan Teknik Mesin Xiii (SNTTM Xiii)*
- [14] Muhammad, H., & Widodo, W. A. (2015). Studi Eksperimental Pengaruh Penggunaan Inlet Disturbance Body Terhadap Karakteristik Aliran Melintasi Silinder Sirkular Yang Tersusun In-Line Square. *Seminar Teknologi Dan Rekayasa (Sentra)*.
- [15] Rina, R., & Ardhy, S. (2018, October 29). Pengaruh Silinder Downstream terhadap Karakteristik Aliran Silinder Upstream Menggunakan Square Disturbance Body Tersusun Tandem. *Jurnal Energi Dan Manufaktur*, 11(2), 58. <https://doi.org/10.24843/jem.2018.v11.i02.p05>
- [16] Fox, R. W., McDonald, A. T., & Pritchard, P. J. (2008, January 1). *Introduction to Fluid Mechanics*. John Wiley & Sons.
- [17] Munson, B. R., Young, D. F., & Okiishi, T. H. (2005, March 11). *Fundamentals of Fluid Mechanics*. Wiley.